Available online at www.sciencedirect.com
ScienceDirect
Journal of Power Sources 175 (2008) 644–650
JOURNAL OF POWER SOURCES
www.elsevier.com/locate/jpowsour

Evaluation of carbon cryogels used as cathodes for non-flowing zinc–bromine storage cells

David Aymé-Perrot [a,*], Serge Walter [a], Zelimir Gabelica [a], Sabine Valange [b]

[a] *Groupe Sécurité et Ecologie Chimiques (GSEC), ENSCMu, 3 rue Alfred Werner, F-68093 Mulhouse Cedex, France*
[b] *Laboratoire de Catalyse en Chimie Organique (LACCO), ESIP, 40 Avenue du Recteur Pineau, F-86022 Poitiers Cedex, France*

Received 26 April 2007; received in revised form 7 September 2007; accepted 16 September 2007
Available online 2 October 2007

Abstract

Monolithic megaloporous carbon cryogels were examined for their potential applications as cathodic electrodes in secondary zinc–bromine cells. This work investigates the possibility of using their particular macroporous texture as microscopic bromine tanks in a zinc/bromine battery. The electrochemical behaviour of a cell based upon such a Br_2 electrode was studied and discussed in terms of energy yields, energy storage capability and cycle life. Good storages (over 20 Wh kg^{-1}) could be obtained during the first 2 h of cell charging for currents between 10 and 20 mA g^{-1}. The energy yield remains almost constant during a fairly large number of cycles, basically for weak charges (e.g. 25 C g^{-1}). Our findings show that the good cyclability of the cathodic electrode is a consequence of the liquid state of the active bromine phase.

Keywords: Zinc–bromine cell; Megaloporous carbon cryogels; Energy storage

1. Introduction

The zinc–bromine system is still considered as to be highly attractive for energy storage purposes since it displays a very high theoretical energy density close to 440 Wh kg^{-1}.

The overall cell reaction is as follows:

$$Zn^{2+} + \underset{\text{(discharged)}}{2Br^-} \leftrightarrow \underset{\text{(charged)}}{Zn + Br_2} \quad (1)$$

The cell e.m.f. calculated from the normal potentials ($E^0_{Zn^{2+}}$ and $E^0_{Br^{2+}}$) is equal to:

$$E = E^0_{Br^{2+}} - E^0_{Zn^{2+}} = 1.06 + 0.76 = 1.82\,V \quad (2)$$

The theoretical specific energy of the $ZnBr_2$ system (440 Wh kg^{-1}) and its practical value (60 Wh kg^{-1}) were compared by Beck and Rüetschi to similar battery systems such as Zn–MnO_2, Ni–Cd, Ni–MH, Li-ion and many others [1] and their respective values were reviewed and thoroughly discussed in the light of their potential new applications (Table 1 in ref. [1]).

Much research has been carried out in order to obtain efficient Zn–Br_2 batteries. Nevertheless, several technical problems which arose, mainly related to bromine diffusion towards the zinc electrode (due to its solubility in water correlated with Br_3^- and Br_5^- formation), but also to zinc dendrite formation, could not be completely solved so far. Several technical solutions were suggested to improve lifetime and reliability of this system, such as the use of Br_2 complexing agents [2,3], or the use of organic solvents to keep the bromine out of the aqueous phase [4,5]. Both techniques were then coupled in order to avoid as much as possible bromine diffusion in the aqueous phase by creating a non-aqueous polybromide phase [6–11]. Most often, these techniques have been developed using an electrolyte circulating system [11] which notably improves the quality of zinc plating. Presently, the zinc bromine battery is constituted of tanks that supply the reaction cell with the cathodic liquid (catholyte) and anodic liquid (anolyte). Although high self-discharge rates and poor cycling capability still hinder the industrial development of such kind of storage cells, these problems are beyond the scope of this study.

The aim of this work was to evaluate the possibility of storing liquid bromine within a carbon cryogel electrode, and to examine the capability of such a material to contribute to solve some aspects of the problems mentioned above.

* Corresponding author. Tel.: +33 617347297; fax: +33 389336815.
E-mail addresses: david.ayme-perrot@uha.fr (D. Aymé-Perrot), serge.walter@uha.fr (S. Walter), sabine.valange@univ-poitiers.fr (S. Valange).

0378-7753/$ – see front matter © 2007 Elsevier B.V. All rights reserved.
doi:10.1016/j.jpowsour.2007.09.076

Several kinds of carbon materials made from resorcinol–formaldehyde aqueous gels have been developed since their introduction in 1989 by Pekala and Kong [12]. Because of their important porosity and high specific surface area, aerogels (supercritical drying) [12–14], xerogels (evaporative drying) [15–17] and cryogels (freeze drying) [18–20] appear to be very attractive materials for numerous applications as electrodes. Presently, they are being already developed for double-layer (EDL) capacitor applications. Similarly, they also show interesting properties for storage battery applications.

Concerning the carbon cryogels, several studies related to freeze drying [21,22], showed that under well defined conditions, huge channels can be generated in the material, leading to a very special kind of macroporosity currently referred to as "megalopores" [18,19]. Such a honeycomb-type texture seems to be difficult to manufacture into reproducible bulk components. Due to their very low density and their important void volume, one generally prefers to grind cryogels and to mix them with carbon black and a binder to form more compact electrodes. However, doing so results in the destruction of the macroporous network which is a highly interesting characteristic of this material.

One could therefore expect, on one hand, the macroporosity (carbon capillary structure) to act as a good bromine storage tank and, on the other hand, the high specific surface area of the bulk material to lead to efficient charge transfer properties.

2. Experimental

2.1. Preparation of RF cryogels

RF gels were synthesized by aqueous sol–gel polycondensation of resorcinol (R) with formaldehyde (F), with sodium carbonate (C) as basification agent, as reported by Pekala et al. [12,13]. Resorcinol (purity > 98%) and sodium carbonate (purity > 99%) were purchased from Acros, while formaldehyde (36.5% in water, methanol-stabilized) was supplied by Riedel de Haën. All products were used as received. A typical gel formulation corresponding to 5% of solid by weight dispersed in distilled water is based on R/F and R/C molar ratios of 0.5 and 50, respectively. The mixture was stirred for 20 min and then poured into cylindrical borosilicate glass (Pyrex) test tubes which were torch-sealed and heated in an oven for gelation at 85 °C for 7 days. The gelation yields a wet product which requires drying before any further use. After the polymerisation process, the solid samples were extracted from the sealed test tubes for drying. Several authors [23–25] suggest to exchange water with *t*-butanol prior to freeze drying in order to prevent the megaloporous structure from cracks due to ice crystal growth. The gels described in this work were not *t*-butanol exchanged but were directly immersed into liquid nitrogen until the nitrogen boiling became gentle. Choosing such a fast cooling procedure (liquid nitrogen or dry ice–acetone) results in the formation of parallel tubular hole structured materials, as described by Mathieu et al. [18]. Since the formation of such a structure was our aim, the liquid nitrogen cooling procedure seemed to be best suited for the intended use. The cold samples were transferred to a CHRIST ALFA freeze drier and dried until constant weight (after nearly 24 h at about 0.04 mbar). The final carbon cryogel was obtained by pyrolysing the dry precursor under nitrogen flow (about 0.1 L min^{-1}) in a horizontal cylindrical oven (diameter: 60 mm) heated up to 1000 °C at 2 °C min^{-1} and kept at 1000 °C for 1 h.

2.2. Material characterisation techniques

The pyrolysed cryogel surface area and pore size analysis were measured by adsorption–desorption of nitrogen on a MICROMERITICS ASAP 2010 instrument (−196 °C). Prior to N_2 adsorption, the samples were degassed under vacuum at 90 °C for 1 h followed by a further heating at 350 °C for 3 h. The BET surface areas were evaluated from the linear part of the BET plots. The pore texture and surface morphology of the samples were visualised by scanning electron microscopy (SEM) with a FEG SUPRA 35-ZEISS microscope. The samples did not require vacuum gold deposition because of their good conductivity, and could be observed in their original state.

2.3. Development of the electric power cell

The cell used for this study has been designed as shown in Fig. 1. In the cathodic compartment, the carbon cryogel electrode was held on a vitreous carbon slice used as current collector. The anode was made of a bulk zinc electrode fitted in a bromine resistant Teflon cell as described by Fig. 1. The electrode separator was made of a 100 μm non-woven glass fibre fabric, thick enough to avoid any short circuit between the electrodes and simultaneously to give the structure some elasticity for an appropriate compensation of the changes in the volume during the charge–discharge cycles, and to provide good electrical contacts on all required interfaces. Polyacrylamide gel was added in order to reduce the diffusion of bromine towards the zinc electrode. More specifically, since the carbon electrode cannot be welded to the metallic current collector, the contact is obtained by means of the slight pressure resulting from the presence of a weak spring above the zinc electrode, as shown by Fig. 1. The apparent surface area of the cathode was 10 cm^2 for a thickness of 2 mm, corresponding to a total cell weight of 10 g.

Such a design enabled us to check whether the tubular carbon cryogel was capable to retain the contained bromine with

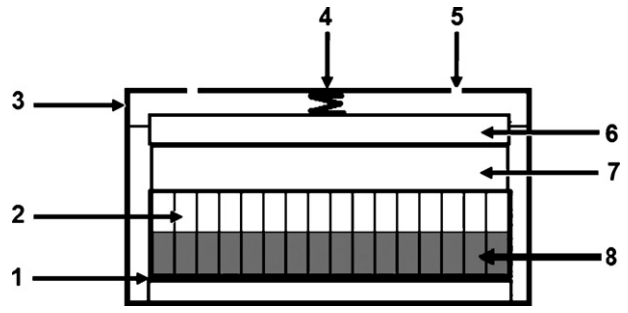

Fig. 1. Modified cell design: (1) platinum grid current collector, (2) carbon cryogel cathode, (3) casing, (4) spring, (5) gas vent, (6) zinc anode, (7) separator. Molecular bromine generated in the $ZnBr_2$ aqueous phase (8).

sufficient efficiency to avoid the self-discharge of the cell due to zinc corrosion by bromine diffusion.

Note that the macropores of the carbon cryogel electrode are oriented perpendicularly to the collectors. In good agreement with the observations made by Mathieu et al. [18], the orientation of the megalopores could be induced during the drying step by a temperature gradient applied across the sample in the desired direction.

In a previous work, Zito [11] studied the correlated variation of bromine solubility and the ionic resistivity of zinc bromide solutions. From his study (ref. [11]; Fig. 7) the highest conductivity is obtained for a zinc bromide molarity close to 2 mol L^{-1}. Oppositely, the lowest value of bromine solubility is reached for zinc bromide concentrations above 7 mol L^{-1}. On one hand, the conductivity must be kept as high as possible in order to reduce to an acceptable value the internal ohmic energy losses of the cell at high discharge rates. On the other hand, low bromine concentrations in the electrolyte are a trend since they result in low corrosion rates of the anodic zinc electrode, whereas the elemental bromine required for energy storage must be kept as far as possible as a separate liquid phase within the megaloporous structure. Keeping in mind that the zinc corrosion kinetics is not in the focus of this study, the first requirement suggests to maintain the zinc bromide molarities as low as 2 mol L^{-1}, while the second trend would require the highest possible zinc bromide concentrations. A good mean path could be to adjust the molarity close to 5 mol L^{-1}, since it corresponds to nearly half of the optimal value both for the conductivity and for the bromine solubility.

Data from Zito (ref. [11]; Figs. 6 and 7) allowed us to recalculate the energy densities and plot their values along with the ionic resistivity data taken from Fig. 7 in ref. [11], against the zinc bromide solution molarity (Fig. 2). Low resistivities will result in low energy losses at high powers. At the minimum of electrical resistivity, which corresponds to about 2 M zinc bromide electrolytes, the energy density is close to 140 Wh kg^{-1}, that is about one-third of the theoretical maximum. Increasing electrolyte molarity gives rise to higher energy densities, but also increases the energy loss at maximum power by a factor proportional to the square of the electrical resistivity, due to the fact that the cell resistance will generate power losses both during the charge and the discharge process, the overall yield being the product of both processes. The grey area in Fig. 2 shows the molarity range of zinc bromide where the electrical resistivity is comprised between the minimum value (about 2.4 Ω in.) and a resistivity higher by a factor of $2\sqrt{2}$ (about 6.8 Ω in.), that is a resistivity leading to identical losses for $(2\sqrt{2})^2 = 8$ times lower power rates. Higher zinc bromide molarities, although increasing the energy densities, would also increase so drastically the power losses at high power rates that such cells would loose most of their interest. A 5 M solution provides a good mean path between the energy density and the conductivity of the electrolyte since it reduces by a factor by two the electrical resistance (and therefore by a factor by 4 the losses at identical power rate) of the cell, although the energy density is just reduced by about 17% with respect to the maximum energy density obtainable within the grey area of Fig. 2. This is due to the increasing density of zinc bromide solutions with increasing molarity. Zinc bromide molarities higher than 7 mol L^{-1} result only in a poor improvement of the energy density, while the rapidly increasing resistivity will drastically drop the energy yield within the same concentration range.

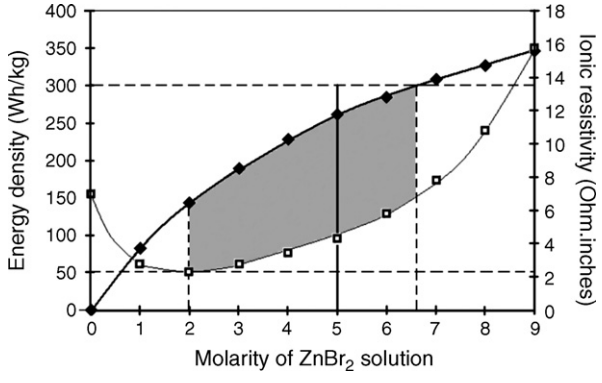

Fig. 2. Energy density (Wh kg^{-1}) (♦) and ionic resistivity (□) of $ZnBr_2$, as a function of $ZnBr_2$ concentration ($T = 293$ °K).

The electrical conductivity of the electrolyte was enhanced through adding ammonium chloride (5 mol L^{-1}).

2.4. Electrochemical characterisation

All the electrochemical experiments related to the study of the charge–discharge cell behaviour have been performed with a Radiometer Analytical VOLTALAB PGZ 100. Galvanostatic tests were carried out using four different current densities, namely 5, 10, 20 and 40 mA g^{-1} (or mA cm^{-2} for the active electrode surface area used here), the density for the discharge process being always the same as for the charge process. The details of the relevant experiments are specified in the context of the results. The charge was conducted so as a cut potential of 2 V is not overstepped. For each of the four current densities, cyclabilities of 25, 50 and 100 C g^{-1} have been selected, knowing that the charging limit of the cell is close to 200 C g^{-1}.

3. General considerations regarding zinc–bromine cells

Discussing the results of this work first requires a reminding of some particular features regarding the zinc–bromine cells.

Bromine is a very reactive element with a high standard potential, corresponding to a fast system with the bromide ion, which makes it very attractive for uses in battery applications. Besides these advantages exist some serious drawbacks, resulting especially from bromine solubility in aqueous systems as well as from its high volatility. These parameters lead to diffusion phenomena towards the zinc electrode where even small amounts of elemental bromine will cause formation of zinc bromide by chemical corrosion. Concerning the techniques proposed to reduce zinc corrosion (bromine complexation and flow cells), one must be aware of the fact that an efficient complexation drastically decreases the activity of bromine. Due to the fact that the bromine/bromide system is fast, the concentration of free bromine must be extremely low at the zinc electrode in order to

result in zinc electrode lifetimes compatible with a practical use (generally several years). But reducing the free bromine concentration by a factor by 10 reduces the cell voltage by 0.06 V. In order to increase the time constant from about 1 h up to 10 years, one must decrease the free bromine concentration by the same ratio, that is almost by a factor by 10^5. Thus, the final cell voltage would be decreased by 300 mV, corresponding to nearly 17% of its initial energy. Moreover, complexation does not actually reduce the concentration of the available bromine capable of corroding the zinc electrode. Complexing the free bromine will store it in a buffer from which it will be released at the same rate as the rate of its consumption from the electrolyte through the corrosion process. That is the main reason why we tried to retain, by a physical method rather than by using some chemical process, as much bromine as possible within the porosity of the carbon-based bromine electrode, by capillary effect trapping.

4. Results and discussion

4.1. Carbon cryogel

Job et al. [22] showed that an important dilution molar ratio $D = 20$ (D = water/{resorcinol + formaldehyde + sodium carbonate}) leads to megalopores or even to fragments depending on the experimental freezing conditions.

Some authors [23–25] prefer applying a *t*-butanol/water exchange step before drying, so as to prevent the gel from cracks due to solvent expansion during freezing. They assume the expansion of water during ice formation to be at the origins of the cracks they could observe in the cryogel tube walls after freeze drying. Such an assumption would mean that the observed cracks are due to the expansion during solidification as a consequence of the lower density of ice than liquid water. This argument leads the authors to prefer replacing water by an organic solvent, that, once frozen, shows a higher density than the liquid phase. Bearing in mind the experiments of Job et al. [22], we came to the conclusion that the main factor ruling the cohesion of the end product after the freezing process, is the solid state crystal size rather than the water expansion, that hardly reaches 10%. Oppositely, increasing the crystal size by a factor by two will result in a crystal volume eight times higher. Thus, it seems reasonable to assume that the use of solvents other than water will result in mechanically stable products more because such solvents yield smaller crystals by freezing than because of their shrinking during solidification.

Even without replacing water by another solvent, fast freezing rates allowed our materials to remain monolithic as previously observed by Mathieu et al. [18]. After pyrolysis, they exhibit a large specific surface area close to 950 $m^2 g^{-1}$. In Fig. 3, SEM micrographs show the material sheet texture with megalopores. After a few cycles, the material texture is partly fragmented (SEM picture not shown), not only because of the possible electrolyte repeated volume variations (see Section 4.3) but also because of the pressure applied to the electrodes during the

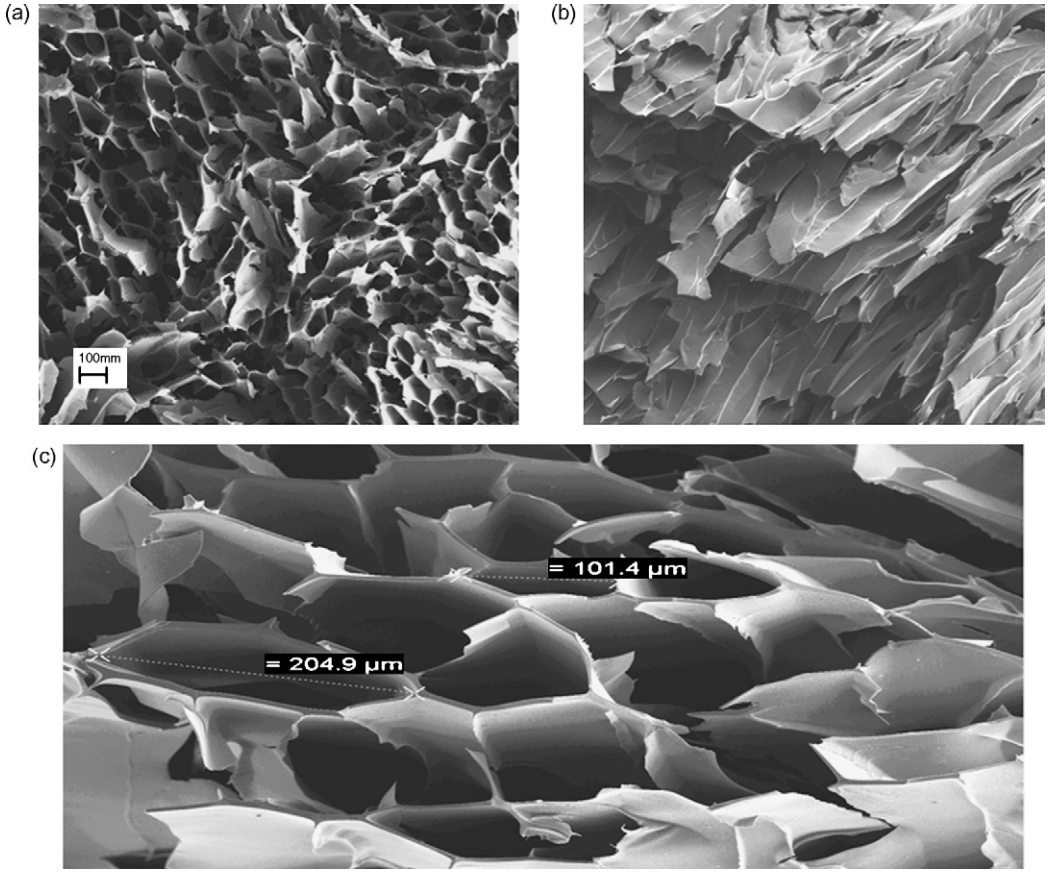

Fig. 3. SEM pictures of the macroporous structure of the carbon cryogel: (a) front view of macropores, (b) macropore sidewalls and (c) macropore sizing.

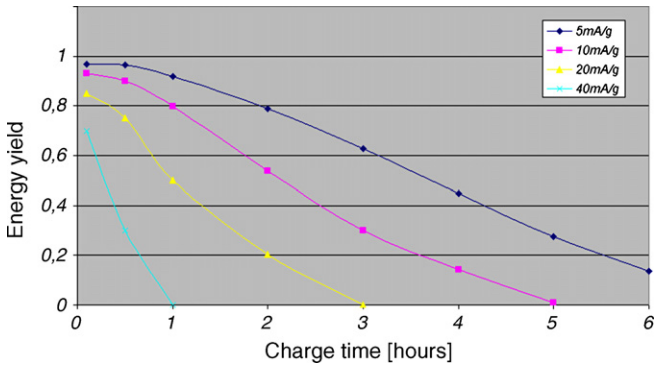

Fig. 4. Energy yield as a function of charge time for various current densities.

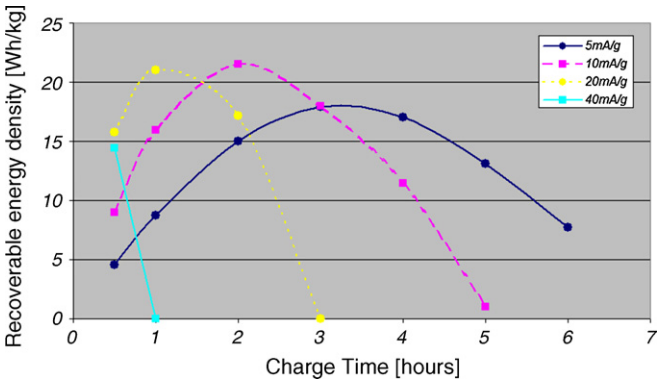

Fig. 5. Recoverable energy density as a function of charge time for various current densities.

electrochemical experiment. Such a partial destruction can be a limitation to a long time use of megaloporous carbon-based materials for durable energy storage purposes. Nevertheless, such a limitation was not observed after a couple of cycles when weak electric charges were applied (see Section 4.3; Fig. 7).

4.2. Energy storage

The cell was tested in the case of the four different current densities (5, 10, 20 and 40 mA g^{-1}), aiming at evaluating the consequent energy yields. Fig. 4 shows, for the four experiments, the energy yield evolution as a function of charge time.

It was observed that, while the yield decreases in each case, this decrease is less pronounced for lower current densities. This can be related to the bromine diffusion rate. A strong current such as 40 mA g^{-1} would generate a large amount of bromine that would not remain for long enough within the megalopores and would therefore further diffuse too rapidly through the carbonaceous material towards the Zn electrode. The excess of anodic bromine will then oxidise chemically part of the cathodic zinc deposit, resulting in a partial self-discharge or, in other words, to a dramatic energy yield decrease.

For this experimental cell, on one hand, the current collector of the carbon cathode was made of glassy carbon in order to prevent its corrosion by bromine. On the other hand, zinc plays a dual role of anode and current collector. As a consequence, both current collectors exhibit a weak overpotential resulting, respectively, in the formation of oxygen and hydrogen bubbles that is increasing with the current density. This is one of the reasons why the energy yield markedly drops for high current values.

For low current densities, these phenomena are substantially slowed down and the energy yield decrease is less pronounced.

The energy yield can be straightforwardly related to the amount of energy recoverable from the system at a given charge–discharge current density. Fig. 5 shows the evolution of the recoverable energy density as a function of the charge time for different current densities.

Fig. 5 provides implicit information concerning the influence of the charge–discharge current density as well as of the total amount of charges stored, on the recoverable energy density of the cell.

Energy density maxima are observed for all systems except the one involving a 40 mA g^{-1} current. The highest energy density (21.5 Wh kg^{-1}) is obtained for a 10 mA g^{-1} current after 2 h charging, corresponding to 72 C g^{-1}. However, the yield at that stage is rather poor (0.54, as shown in Fig. 4). Higher yields can only be obtained for shorter charging times.

The shape of each curve in Fig. 5 is due to a simultaneous influence of two effects, namely a preliminary increasing charge (the recoverable energy is a function of charge density) followed by an energy decrease due to bromine diffusion. Bromine diffusion occurs from the bromine electrode to the Zn cathode because of an increased amount of Br_2 produced. Indeed, during the early steps of the charging process, only small amounts of bromine start to diffuse towards the zinc electrode. Zinc corrosion starts as soon as some bromine is lost by the increasing diffusion process. The diffusion increases with the amount of stored bromine with, as a result, a consequent recoverable energy decrease in the late steps of the process. The rapid decrease of the recoverable energy beyond the maxima is clearly related to the increasing bromine diffusion rate with increasing charge.

Bromine diffusion is a very disturbing phenomenon, not easy to overcome. It may be due to the formation of soluble bromine transferring ions such as Br_3^- and Br_2Cl^- and more complex polyatomic structures, the existence of which has been thoroughly described [26,27]. The main disadvantage of bromine is that it remains almost completely insulating because of its covalent state. Only the soluble ionic species such as Br^{3-} or Br_2Cl^- can be electroactive on the carbon electrode surface with respect to the reduction of elementary bromine to bromide. Thus the presence of bromide and chloride ions in the aqueous phase is a must in order to achieve a sufficiently large electroactivity of bromine. Zinc bromide and, to a lesser extent, ammonium chloride must therefore remain present at high concentrations in the electrolyte. But in the same time this will result in the presence of highly chemically active bromine present all through the aqueous electrolyte from the bromine to the zinc electrode. Only the amount of bromine exceeding the saturation of the electrolyte can be stored in the elemental state within the bottom side of the cryogel pores. Therefore, it might be difficult to keep the zinc corrosion by bromine diffusion at a sufficiently low rate for long life practical applications.

Self-discharge by zinc corrosion occurs as soon as elemental bromine is present somewhere in the cell. Charging the cell is only possible with current densities exceeding the self-discharge rate. Moreover, since self-discharge by zinc corrosion due to diffusing bromine goes on whether the cell is being charged, discharged or kept under open circuit. Therefore, the total time from the beginning of the charging process to the end of the discharging process will be extremely significant concerning the apparent performance of the device. That is one main reason why the charging step could not be prolonged beyond 2 h when using a 10 mA g^{-1} current density (Fig. 5) since an increasing amount of bromine within the carbon porosity would lead to increasing diffusion rates towards the zinc electrode. As a consequence, a fast zinc electrode corrosion was observed, a phenomenon directly correlated to poor energy yields. This is further confirmed by the use of a current density of 20 mA g^{-1}: while the maximum energy stored was attained after only 1 h, a prolonged charging at the same rate would rapidly lead to a sharp energy drop because of an almost complete bromine creeping towards the Zn electrode. This means that at such charge times, a steady state is reached once the bromine diffusion rate has become as high as the bromine generation rate resulting from the charging process. This factor is strongly dependent on the geometrical design of the cell, and more specifically, on the thickness and fabric density of the non-woven separator used in the electrolyte filled interval between cathodic and anodic electrodes of the cell.

As a preliminary conclusion, Fig. 5 shows the ability of our cell to store energies larger than 20 Wh kg^{-1}, at least for medium current densities. Nevertheless, interesting yields can still be obtained at high charge–discharge current densities (about 10 times higher than for conventional lead batteries), provided the cell is operating far from its maximum charge capabilities.

4.3. Cell cycle life

The cycle life of our system is illustrated in Fig. 6 for the three different charge densities considered (25, 50 and 100 C g^{-1}) in the case of the four charge–discharge current densities.

Logically it was observed that the number of charge–discharge cycles increases with the decreasing current density. Short cycling is observed when bromine is either rapidly generated (40 mA g^{-1}) or extensively accumulated (charge

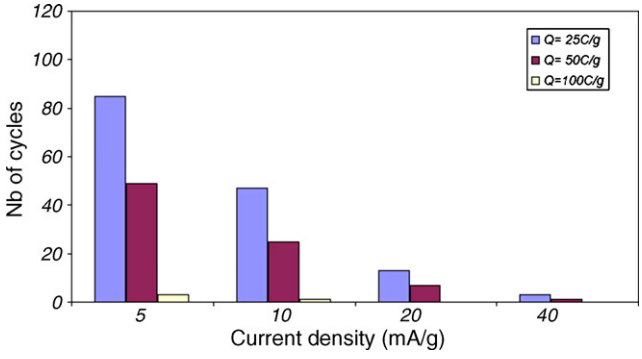

Fig. 6. Number of cycles as a function of current density for three different charge densities applied to the cell.

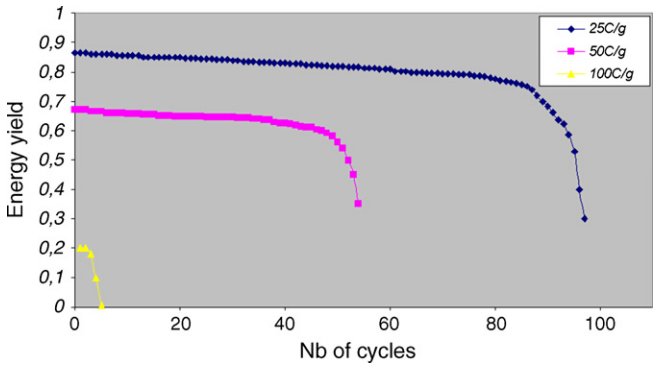

Fig. 7. Energy yield as a function of number of cycles, for three different charge densities applied to the cell for a current of 5 mA g^{-1}.

density of 100 C g^{-1}). A current of 5 mA g^{-1} allowing 47 charge–discharge cycles for a charge 50 C g^{-1} could be an acceptable compromise. The same number of cycles can be achieved with 10 mA g^{-1} but, in that case, the charge density is only about one half (25 C g^{-1}).

As seen before, the energy yield decreases as a function of charge time, or, in other words, of the stored charge. Fig. 7 shows, for the same three different charge densities, the evolution of the energy yield versus the number of cycles in the case of a charge–discharge current of 5 mA g^{-1}.

The yield remains almost constant during a large number of cycles, especially for weak charges (e.g. 25 C g^{-1}) and then very rapidly drops. This drop can be explained by considering that a certain amount of bromine that neither reacted on the cathode interface nor on the Zn anode (self-discharge) would accumulate, with cycle time, inside the cathode megaloporous volume. The resulting important electrolyte molar volume variation can then be responsible for the electrode eventual damage at the end of the process. Another way to explain the damage is to assume that electrolyte volume variations during each cycle provoke repeated mechanical stresses that eventually lead to the carbon electrode partial or even total collapse. Such a partial collapse as observed by SEM for long cell life times (micrograph not shown) can therefore stem from both mechanical pressure during cell shaping and electrolyte repeated volume variations.

This yield variation with the cycle life justifies that the energy yields reported in Fig. 4 were measured after the first cycle for each period of time.

5. Conclusion

This work shows that megaloporous carbon cryogels used as cathodic material of a zinc bromine secondary cell are capable of storing reversibly substantial amounts of elemental bromine. The highest energy (21.5 Wh kg^{-1}) was recovered from the cell upon using a 10 mA g^{-1} current after 2 h charging.

Such a specific energy still remains small when compared with the theoretical value which is theoretically higher than 260 Wh kg^{-1} under our experimental conditions ($ZnBr_2$: 5 M). However, it is close to the energy density of commonly used lead batteries but obtained with current densities about 10 times higher.

Short cycling was observed when bromine is either rapidly generated (current of 40 mA g^{-1}) or extensively accumulated inside the cathode (charge density of 100 C g^{-1}), thereby suggesting that a current of 5 mA g^{-1} allowing about 50 charge–discharge cycles for a charge density of 50 C g^{-1} could be a fair compromise for an acceptable energy storage (about 17.5 Wh kg^{-1}).

The recoverable energy yield remains almost constant during a fairly large number of cycles, basically for weak charges (e.g. 25 C g^{-1}). For high charges, the yield very rapidly drops due to electrode damage provoked by repeated mechanical stress induced by electrolyte molar volume variations during the cycle life.

Such drawbacks can be possibly avoided by only partly filling (not over 70%) the cathode megalopores by the electrolyte as the electrochemical reaction essentially takes place next to the upside-turned windows of the parallel megalopores, thus closer to the zinc electrode. In such a case, nearly half of the macroporous volume is filled with the 5 M zinc bromide solution and would allow the aqueous reversible $2Br^-/Br_2$ electrochemical reaction to occur.

Acknowledgements

We wish to acknowledge the "Ministère de l'Education Nationale, de la Recherche et de la Technologie, Région Alsace, Conseil Général du Haut-Rhin" and the "Communauté des Communes Mulhouse Sud-Alsace", for their financial support.

References

[1] F. Beck, P. Rüetschi, Electrochem. Acta 45 (2000) 2467.
[2] D.J. Eustace, J. Electrochem. Soc. 119 (1980) 528.
[3] M. Mastragostino, S. Valcher, Electrochim. Acta 28 (1983) 501.
[4] P. Singh, K. White, A.J. Parker, J. Power Sources 10 (1983) 309.
[5] P. Singh, J. Power Sources 11 (1984) 135.
[6] K.J. Cathro, K. Cedzynska, D.C. Constable, P.M. Hoobin, J. Power Sources 18 (1986) 349.
[7] K.J. Cathro, J. Power Sources 23 (1988) 365.
[8] G. Bauer, J. Drobits, Ch. Fabjan, H. Mikosch, P. Schuster, Chem. Ing. Tech. 68 (1996) 100.
[9] G. Bauer, J. Drobits, Ch. Fabjan, H. Mikosch, P. Schuster, J. Electroanal. Chem. 427 (1997) 123.
[10] W. Kautek, A. Conradi, M. Sahre, Ch. Fabjan, J. Drobits, G. Bauer, P. Schuster, J. Electrochem. Soc. 146 (1999) 3211.
[11] R. Zito Jr., US Patent 4,482,614 (1984).
[12] R.W. Pekala, F.M. Kong, Rev. Phys. Appl. 24 (1989) 33.
[13] R.W. Pekala, C.T. Alvisio, J.D. LeMay, J. Non-Cryst. Solids 125 (1990) 67.
[14] R.W. Pekala, US Patent 4,997,804 (1991).
[15] C. Lin, J.A. Ritter, Carbon 35 (1997) 1271.
[16] N. Job, F. Panariello, J. Marien, M. Crine, J.P. Pirard, A. Léonard, J. Non-Cryst. Solids 352 (2006) 24.
[17] A. Léonard, N. Job, S. Blacher, J.P. Pirard, M. Crine, W. Jomaa, Carbon 43 (2005) 1808.
[18] B. Mathieu, B. Michaux, O. Van Cantfort, F. Noville, R. Pirard, J.P. Pirard, Ann. Chim. Sci. Matér. (Paris) 22 (1997) 19.
[19] B. Mathieu, S. Blacher, R. Pirard, J.P. Pirard, B. Sahouli, F. Brouers, J. Non-Cryst. Solids 212 (1997) 250.
[20] R. Kocklenberg, B. Mathieu, S. Blacher, R. Pirard, J.P. Pirard, R. Sobry, G. Van den Bossche, J. Non-Cryst. Solids 225 (1998) 8.
[21] H. Nishihara, S.R. Mukai, H. Tamon, Carbon 42 (2004) 885.
[22] N. Job, A. Théry, R. Pirard, J. Marien, L. Kocon, J.N. Rouzaud, F. Béguin, J.P. Pirard, Carbon 43 (2005) 2481.
[23] H. Tamon, H. Ishizaka, T. Yamamoto, T. Suzuki, Carbon 38 (2000) 1099.
[24] T. Yamamoto, T. Nishimura, T. Suzuki, H. Tamon, J. Non-Cryst. Solids 288 (2001) 46.
[25] O. Czakkel, K. Marthi, E. Geissler, K. László, Microporous Mesoporous Mater. 86 (2005) 124.
[26] F.A. Cotton, G. Wilkinson, Advanced Inorganic Chemistry, fourth ed., Wiley, New York, 1980, p. 567.
[27] A.J. Bard, Encyclopaedia of Electrochemistry of the Elements, vol. 1, Dekker, New York, 1973, p. 59.